Serb. Astron. J. № 169 (2004), 53 - 58 **UDC 52.47**
Original scientific paper

ELECTRON ENERGY-LOSS SPECTROSCOPY OF AUTOIONIZING STATES OF ZINC

B. Predojević[1,2], D. Šević[1], V. Pejčev[1,3], B. P. Marinković[1] and D. M. Filipović[1,4]

[1] *Institute of Physics, PO Box 57, 11001, Belgrade, Serbia and Montenegro*

[2] *Faculty of Natural Sciences, University of Banja Luka, Republic of Srpska, Bosnia and Herzegovina*

[3] *Faculty of Natural Sciences, University of Kragujevac, Serbia and Montenegro*

[4] *Faculty of Physics, University of Belgrade, PO Box 368, 11001, Belgrade, Serbia and Montenegro*

(Received: September 15, 2004; Accepted: October 4, 2004)

SUMMARY: Autoionizing energy-loss spectra of Zn from 10.8 to 12.5 eV, for incident electron energies between 20 and 100 eV, have been recorded at scattering angles from 0° to 10°. These spectra were decomposed using χ^2 minimization procedure to show the contribution of the $3d^{10}4s^2 \rightarrow 3d^9 4s^2 4p$, single inner-electron transitions. Relative intensities of lines in the Zn spectra are determined with respect to the $3d^{10}4s^2 \rightarrow 3d^{10}4s4p$ resonance line. The line shapes and widths are examined. The results are compared with available measurements and theoretical estimates.

Key words. Atomic processes - Scattering - Line: profiles

1. INTRODUCTION

Line intensities in autoionizing spectra of atoms for both "optically allowed" and "optically forbidden" transitions are of importance for determination of physical constants in astrophysical plasmas (Doschek 1985). Ionization process via autionization could be in many cases more important than the direct one.

Single inner-electron transitions $3d^{10}4s^2 \rightarrow 3d^9 4s^2 np$ (where $n \geq 4$) are dominant in autoionizing spectra of Zn. The transitions were initially observed in photoabsorption spectra by Beutler (1933) and Beutler and Guggenheimer (1933). Garton and Connerade (1969) investigated the absorption spectra of Zn single inner-electron transitions in the region from 13.7 to 20.6 eV and gave considerable extension of the early results by Beutler. The obtained spectra contain states belonging the d^9s^2np, nf series and classified in the J_cK coupling scheme. Marr and Austin (1969) measured absolute cross sections for photoabsorption, that causes both ionization and autoionization, from the ionization threshold (IP=9.39 eV) to 16.53 eV, emphasizing the role of the $3d^9 4s^2 np$ autoionizing states. In the Zn spectra, Mansfield and Connerade (1978) found many regularities that are similar to those in Cd, except that the lines in Zn are much closer to each other. Also, the strong perturbation of high series members of the double valence excitation spectrum by single inner-electron transitions to the $3d^9 4s^2 5p$ autoionizing states in Zn was found. Chantepie et al. (1988) and Cheron et al. (1991) investigated level widths of $4p^2$ autoionizing states using laser excitation from the $4s4p^3P_J$ levels.

Study of ejected-electron spectra resulting from electron excitation of Zn autoionizing levels has been reported by Back et al. (1981). At incident electron energies E_0=16-300 eV they observed 83 autoionizing levels of Zn and Zn II. The spectra have been observed at 60° with respect to the direction of the incident beam. Energy-loss spectra of the Zn autoionizing states are restricted to those recorded by Trajmar and Williams (1976). In energy-loss spectra, beside optically allowed transitions, forbidden transitions are also visible. In these spectra taken at lower electron impact energies and larger scattering angles, forbidden transitions could dominate over optical allowed transitions. On the contrary, spectra taken at higher impact energies and small scattering angles are referred to as "optical-like" spectra and they closely resemble the photoabsorption spectra. On the other side, in the optical spectroscopy the resolution is much better in comparison with electron spectroscopy.

The autoionizing (n-1)d^9ns^2mp (m=4,5,6) energy levels of Zn, Cd and Hg have been calculated by Martin et al. (1972) using various methods including Hertree-Fock (HF) and intermediate-coupling scheme. For the same atoms, Martin (1984) obtained the Slater-Condon parameters from experimental energy levels and optical oscillator strengths (OOS) and calculated energy levels using the single configuration approximation. Mansfield (1981) used multiconfiguration Hertree-Fock (MCHF) method to interprete the electron-ejected spectra by Back et al (1981). Stevanović et al. (2003) used multiconfiguration Dirac-Fock (MCDF) method to calculate energies of the $3d^94s^24p$ components, without taking the connection of discrete states with continuum into account.

Experimental conditions pertaining to the metal-vapor source and characteristics of the electron optics relevant for quality of the spectra are included in Section 2. Results of the energy-loss measurements and decomposed energy-loss spectra are shown and discussed in Section 3. Finally, conclusion is given in Section 4.

2. EXPERIMENT AND PROCEDURE

The apparatus used in this work is the electron spectrometer described earlier (Predojević et al. 2003). Briefly, the optics of both the monochromator and the analyzer are very similar to that designed by Chutjian (1979). Doppler broadening of lines in electron energy-loss spectra is minimized because the electron beam is perpendicular to the atomic beam and because of the narrow beam geometry. All cylindrical electrostatic lenses are made of gilt oxygen-free high-conductivity copper, while hemispherical energy selectors and diaphragms are made of molybdenum.

The spectrometer operates in energy-loss mode, which means that for a given incident electron energy, an addition of energy to the inelastically scattered electrons is achieved by sweeping the analyzer potential. If the addition of energy is equal to the energy-loss of the incident electrons in a particular scattering process, such electrons will pass trough the analyzer and will be detected by a channel electron multiplier. The analyzer can be positioned from -30° up to 150° with respect to the mechanical zero. At given scattering angle (θ) and E_0, energy-loss spectrum was accumulated by multi channel analyzer. Typical overall energy resolution (as FWHM) was 140 meV. The angular resolution of the spectrometer is estimated to be 1.5°. Before each run, the scattered electron intensity was measured from -10° to +10°, so the real zero scattering angle was always determined according to the symmetry of intensity around the instrumental zero. The energy scale was calibrated by measuring the position of the structure at 4.03 eV, attributed to the 4^3P excitation threshold of Zn. (Kazakov 1981)

The metal-vapour source consists of a tubular titanium crucible, which is completely resistive to Zn vapour (Ross and Sonntag 1998). The crucible is placed in a stainless steel cylinder co-axially wrapped with two resistive bifilar heaters (top and bottom) that enable the top of the system to be maintained at approximately 100 K higher temperature than the bottom. This prevents clogging and minimizes dimmer production. Monitoring of the temperature is carried out by two thermocouples, on the top and at the bottom of the crucible. To attain higher ultimate temperature and more stable operating conditions, a titanium foil around the cylinder and tantalum foil on its top end are mounted to reflect the thermal radiation back to the crucible. An additional outer cylinder made of copper serves as a radiation shield and also as a collimator for the metal vapour that turns into the solid state in a liquid-nitrogen cold trap mounted above the interaction region.

Careful choice of the temperature is important because a feature due to double scattering of electrons after excitation of the same $4p(^1P_1)$ resonant state at 5.8 eV, screens the autoionizing features in the vicinity of 11.6 eV. Zn (purity 99.9%) was firstly heated at about 800 K, but temperature was later decreased to 750 K, so that the shape of the autoionizing spectrum was not temperature sensitive. Working temperature corresponded to the metal-vapour pressures of 103 Pa. The atom beam effused through cylindrical channel in the cap with aspect ratio $\gamma = 0.075$.

Lines in the autoionizing spectra of Zn are close to each another, so we performed the decomposition of the unresolved features using the energy levels reported by Mansfield (1981). The fitting function used was Voigt line profile with Gaussian width of 140 meV, except in the case of states at 11.828 and 11.892 eV. These two states were fitted by asymmetric log-normal line profile, because of their obvious asymmetry (Marr and Austin 1969). Finally, lines in the Zn spectra are assigned according to Mansfield (1981) and their relative intensities are determined with respect to the $3d^{10}4s^4p\ 4^1P_1$ resonance state.

3. RESULTS AND DISCUSSION

We have recorded autoionizing energy-loss spectra of Zn at E_0 = 20 eV ($\theta = 6°$ and 10°), E_0 = 60 eV ($\theta = 4°$, 6° and 10°), E_0 = 80 eV (θ = 0°, 4° and 10°) and E_0 = 100 eV ($\theta = 0°$), in the energy-loss region from 10.8 to 13 eV. Energy-loss spectrum at E_0 = 60 eV and $\theta = 4°$ is shown in Fig. 1. Above the ionization potential it contains two features at about 10.98 eV and 11.18 eV and a broad feature at about 11.9 eV. In the energy range from 10.8 to 12.5 eV Mansfield (1981) calculated positions of twelve states belonging to the $3d^{10}4s^2 \rightarrow 3d^9 4s^2 4p$ transitions and one two-valence excited state of the $3d^{10}4p^2$ configuration. Back et al. (1981) detected nine transitions in ejected electron spectra in this energy range. In Table 1, theoretical designation of these states with relative contribution of different configurations according to Mansfield (1981) and respective energy levels are given, together with the observed transitions photoabsorption and ejected electron spectroscopy.

We have decomposed our experimentally obtained energy-loss spectra in the energy range from 11 to 12.4 eV and six autoionizing states were identified. Results of these decompositions at E_0 = 60 eV ($\theta = 10°$) and E_0 = 100 eV ($\theta = 0°$) are shown in Fig. 2. We identified four relatively weak lines with Voigt profile numbered 2, 5, 9 and 10 and two strong lines with asymmetric log-normal profile numbered 11 and 13.

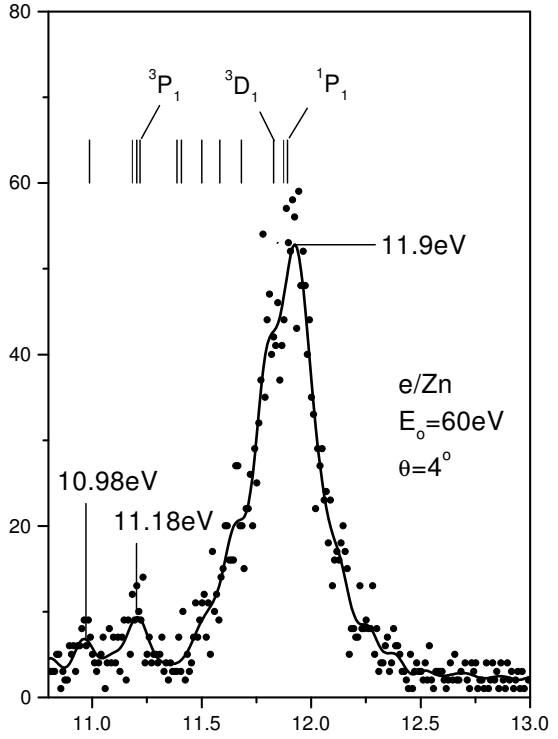

Fig. 1. *Energy-loss spectra of zinc at 60 eV electron impact energy and $\theta = 10°$. In order to show existing structures fast Fourier transform smoothing was applied.*

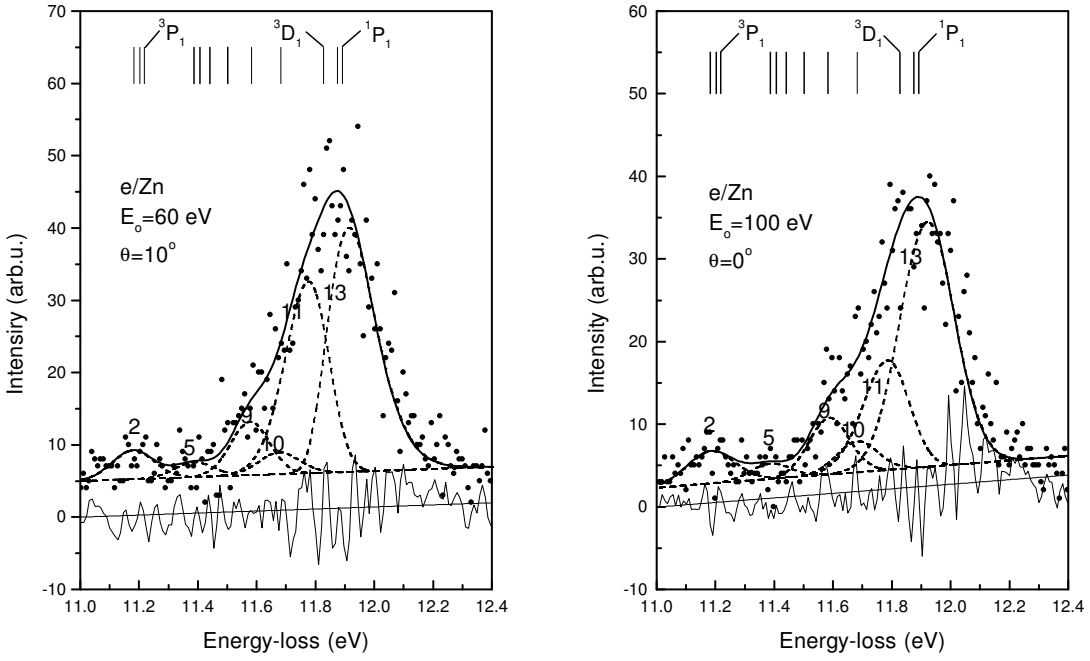

Fig. 2. *Decomposed energy-loss spectra of Zn at E_0 = 60 eV ($\theta = 10°$) and E_0 = 100 eV ($\theta = 10°$): •, row data; - - -, decomposed lines on the baseline (designated in agreement with designation of lines in Table 2.); —, synthetic spectrum. The difference between row data and synthetic spectrum is given at the bottom.*

Table 1. The energy level positions of Zn obtained from theoretical calculation (Mansfield 1981), photoabsorption (Mar and Austin 1969), and ejected electron spectra measurements (Back et al. 1981).

Line No.	Experiments			Theory		
	Back et al. 1981		Marr and Austin 1969	Mansfild 1991		
	Energy (eV)	J	Energy (eV)	Energy (eV)	J	designation
1	10.974	2		10.988	2	$3d^9 4s^2 4p^1(97\%{}^3P + 3\%\ {}^1D)$
2				11.183	3	$3d^9 4s^2 4p^1(64\%{}^3F + 33\%\ {}^1F + 3\%\ {}^3D)$
3				11.203	4	$3d^9 4s^2 4p^1(100\%{}^3F)$
4	11.187	1,3, 4	11.186	11.218	1	$3d^9 4s^2 4p^1(92\%{}^3P + 4\%\ {}^1P + 3\%\ {}^3D)$
5	11.379	0		11.387	0	$3d^9 4s^2 4p^1(99.5\%{}^3P)$
6				11.407	2	$3d^9 4s^2 4p^1(68\%{}^3F + 15\%\ {}^3D + 15\%\ {}^1D + 1\%\ {}^3P)$
7	11.504	2		11.441	0	$3d^{10} 4p^2(99.8\%{}^1S)$
8	11.539	3		11.501	3	$3d^9 4s^2 4p^1(64\%{}^3D + 30\%\ {}^1F + 5\%\ {}^3F)$
9	11.619	2		11.583	2	$3d^9 4s^2 4p^1(49\%{}^1D + 30\%\ {}^3F + 21\%\ {}^3D)$
10	11.669	3		11.682	3	$3d^9 4s^2 4p^1(36\%{}^1F + 33\%\ {}^3D + 31\%\ {}^3F)$
11	11.799	1	11.803	11.828	1	$3d^9 4s^2 4p^1(73\%{}^3D + 20\%\ {}^1P + 6\%\ {}^3P) + 3d^{10} 4s4p(0.5\%{}^1P)$
12				11.875	2	$3d^9 4s^2 4p^1(61\%{}^3D + 36\%\ {}^1D + 2\%\ {}^3P + 1\%\ {}^1F)$
13	11.883	1,2	11.876	11.892	1	$3d^9 4s^2 4p^1(73\%{}^3P + 24\%\ {}^3D + 1\%\ {}^3P) + 3d^{10} 4s4p(2\%{}^1P)$

Table 2. The intensity ratios A_i/A_r (i^{th} over 4^1P_1 resonance state) from decomposed spectra of Zn.

Line No.	The line intensity ratio A_i/A_r								
	E_0=20eV θ=6°	E_0=20eV θ=10°	E_0=60eV θ=4°	E_0=60eV θ=6°	E_0=60eV θ=10°	E_0=80eV θ=0°	E_0=80eV θ=4°	E_0=80eV θ=10°	E_0=100eV θ=0°
1	0.54E-3 (0.28E-3)		1.57E-3 (0.49E-3)						
2	1.43E-3 (0.51E-3)	13.0E-3 (9.7E-3)	2.14E-3 (0.52E-3)	2.69E-3 (1.16E-3)	3.08E-3 (0.76E-3)	0.91E-3 (0.01E-3)	1.83E-3 (0.65E-3)	3.26E-3 (2.96E-3)	4.55E-3 (1.16E-3)
3									
4									
5	0.49E-3 (0.44E-3)	3.06E-3 (2.50E-3)	0.55E-3 (0.36E-3)	0.82E-3 (0.74E-3)	1.49E-3 (0.72E-3)	0.36E-3 (0.02E-3)			1.82E-3 (0.97E-3)
6									
7									
8									
9	2.30E-3 (0.50E-3)	25.1E-3 (3.3E-3)	4.27E-3 (0.53E-3)	7.55E-3 (1.07E-3)	5.31E-3 (0.72E-3)	5.65E-3 (0.02E-3)	9.88E-3 (0.63E-3)	15.1E-3 (6.5E-3)	6.79E-3 0.99(E-3)
10	3.98E-3 (0.49E-3)	22.5E-3 (3.5E-3)	2.28E-3 (0.53E-3)	4.12E-3 (1.36E-3)	2.29E-3 (0.76E-3)	5.89E-3 (0.03E-3)	11.9E-3 (0.6E-3)	27.8E-3 (7.4E-3)	3.81E-3 (1.01E-3)
11	5.37E-3 (0.53E-3)	76.2E-3 (3.9E-3)	15.4E-3 (0.6E-3)	20.8E-3 (1.4E-3)	21.7E-3 (0.8E-3)	7.99E-3 (0.03E-3)	10.1E-3 (0.7E-3)	23.3E-3 (8.6E-3)	15.2E-3 (1.14E-3)
12									
13	11.1E-3 (0.57E-3)	13.4E-3 (0.5E-3)	29.9E-3 (0.6E-3)	30.7E-3 (2.1E-3)	30.8E-3 (0.9E-3)	16.25E-3 (0.03E-3)	32.7E-3 (0.8E-3)	84.0E-3 (8.9E-3)	40.3E-3 (1.4E-3)

According to Mansfield (1981), there are three states at lower energies: 11.183 eV (J=3), 11.203 eV (J=4) and 11.218 eV (J=1). Energy resolution in our measurements was not high enough to resolve these states or to enable decomposition in a unique way. We obtained only one feature (number 2) at energy about 11.18 eV. This value is in good agreement with the result by Back (1981) for J=1,3,4. The states at 11.407 eV (J=2; 68% ^{3}F), 11.441 eV (J=0), 11.501 eV (J=3) and 11.875 eV (J=2; 61% ^{3}D) have not been confirmed in our decomposition procedure. The state number 5 is optically forbidden transition (J = 0 → 0), and consequently was not observed in photoabsorption, but it was present in electron spectroscopy. Also, the state at 11.407 eV was detected neither in photoabsorption measurements and ejected electron spectra and nor in our spectra. The state at 11.441 eV (2.11 eV in ejected electron spectra) is pure $3d^{10}4p^2$ two-valence excited state, absent in photoabsorption spectra. The state at 11.501 eV has appeared only in ejected electron spectra at E_0 =16 eV, but not at energies as high as there in our measurements. Finally, the state at 11.875 has not been detected in photoabsorption measurements and ejected electron spectra. Moreover, this state is very close to the strongest lines at 11.828 eV and 11.892 eV, so that it is probably overlapped.

Trajmar and Williams (1976) reported the Zn energy-loss spectra at E_0 = 20 eV ($\theta = 30°$ and 90°) and 40 eV ($\theta = 10°$). Beside ^{3}P, ^{1}P and ^{3}D series of lines belonging to the $3d^94s^2np$ (n≥4) states, they observed nine other, most probably optically forbidden autoionizing states belonging to the $3d^94s^2nl$ configuration. The feature at 11.60 eV, reported by these authors, obviously appears due to double scattering of incident electrons after successive excitation of the Zn 4^1P_1 resonance state at 5.794 eV. The double scattering in our experiment was avoided by using appropriate temperature of the crucible, as it is explained in Section 2.

Line shapes were examined using Shore profiles in the cases of lines 11 and 13, but deviations of residual functions (difference between raw data and the synthetic spectra) where large, probably due to interference of autoionizing states. Mies (1968) considered interaction between individual states. On the other hand, we used asymmetric log-normal profile for these two states. As a result, we obtained much better fit confirming asymmetry of lines 11 and 13 observed in photoabsorption measurements by Marr and Austin (1969). Taking into account the instrumental broadening in our experiment, we found line widths (Γ) as follows: Γ=175 meV for the line 11, and Γ=200 meV for the line 13. The line width of the four less-intensive lines are much smaller than instrumental broadening, so that their true widths could not be obtained accurately. We estimate that line widths, for the lines denoted by 2, 5, 9 and 10, are about 13 meV.

The intensity ratios A_i/A_r (i^{th} over the 4 $^1P_1$ resonance state) are determined and presented in Table 2, together with estimated uncertainties (in parentheses). Absolute intensities of the resonance state are given recently by Panajotović et al. (2004). These ratios are obtained by dividing the area of decomposed line by the area of resonant one for a particular energy loss spectrum. In energy loss spectrum, the resonant line is observed at 5.79 eV while the autoionization lines of our interest are above approximately 11 eV. For higher electron impact energies (60 eV and above), the difference in residual electron energy is small and, hence, the influence of the transmission is negligible. At these energies our spectrometer was focused at the resonant peak. On the contrary, for smaller electron impact energy (20 eV) this difference is large and the change in analyzer transmission is significant. At this energy, the spectrometer was focused at the most intensive autoionization feature at energy loss of 11.9 eV. Hence, the observed ratios at 20 eV are corrected by the factor of 0.8 according to the transmission measurements by Marinković (1989). At the particular impact energy, from these ratios, one can conclude that differential cross sections of the autoionizing states decrease with increase of the scattering angle less rapidly than those for the resonant state.

It seems that, generally, the intensity ratios A_i/A_r (i-th over the 4^1P_1 resonance state) at θ = 0°, 4°, 6° and 10° increase if the energy increases from 20 to 100 eV. However, A_i/A_r at $\theta = 10°$ decrease, from E_0 = 20 to 60 eV, except for the $^3P_1$ state (at 11.892 eV).

4. CONCLUSION

We have continued a series of electron spectroscopy measurements of electron collisions with IIb group atoms, at low and medium impact energies (Marinković et al. 1991, Panajotović et al. 1993, 2004 and Panajotović 1999). Autoionization region was separately investigated for Zn and Cd atoms by Predojević et al. (2003).

We used the energies of the $3d^94s^24p$ autoionizing states of Zn, calculated by Mansfield (1981), to analyze our energy-loss spectra and to decompose it into six lines. A simple folding of a pure dipole photoabsorption spectrum obtained by Marr and Austin (1969) with a Gaussian of FWHM 140 meV being the resolution in our experiment, cannot reproduce our energy-loss spectra (Predojević et al. 2003). At lower incident electron energies, the autoionizing states with J ≠ 1 contribute to the $3d^94s^24p$ multiplet noticeably, but only tentative assignments of the three states with J=1 are given by Back et al. (1981). According to Mansfield (1981), several autoionizing states are not identified in the ejected-electron spectra and the state at 11.441 eV is practically purely the $3d^{10}4p^2$ ^{1}S (J=0) two-valence excited state. We concluded, from our measurements and analysis, that the states around 11.7 eV with J ≠ 1 also contribute to our energy-loss spectra, in accordance with the low energy ejected-electron spectra. We have determined the intensity ratios of all six identified autoionizing states with respect to the 4^1P_1 resonant state.

Acknowledgements – This work was supported by the project 1424 of MNZŽS, Republic of Serbia, and partly supported by EPIC (Electron Positron Induced Chemistry) European FW5 program.

REFERENCES

Back, C.G., White, M.D., Pejčev, V. and Ross, K.J.: 1981, *J. Phys. B: At. Mol. Opt. Phys.*, **14**, 1497.
Beutler, H.: 1933, *Z. Phys.*, **87**, 19.
Beutler, H. and Guggenheimer, K.: 1933, *Z. Phys.*, **87**, 176.
Chantepie, M., Cheron, B., Cojan, J.L., Landais, J., Laniepce, B. and Aymar, M.: 1988, *J. Phys. B: At. Mol. Opt. Phys.*, **21**, 1379.
Cheron, B., Cojan, J.L. and Landais, J.: 1991, *J. Phys. B: At. Mol. Opt. Phys.*, **24**, 1303.
Chutjian, A.: 1979, *Rev. Sci. Instrum.*, **50**, 347.
Doschek, G.A.: 1985, Autoionozation, Ed. Temkin, A. (New York: Plenum), p. 171.
Garton, W.R. and Connerade, J.P.: 1969, *Astropys. J.*, **155**, 667.
Kazakov, S.M.: 1981, *Pis'ma v ŽTF*, **7**, 900.
Mansfield, M.W.D.: 1981, *J. Phys. B: At. Mol. Phys.*, **14**, 2781.
Mansfield, M.W.D. and Connerade, J.P.: 1978, Proc. R. Soc. A, **359**, 389.
Marinković, B.P.: 1989, PhD Thesis, Faculty of Physics, University of Belgrade.
Marinković, B., Pejčev, V., Filipović, D. and Vušković, L.: 1991, *J. Phys. B: At. Mol. Opt. Phys.*, **24**, 1817.
Marr, G.V. and Austin, J.M.: 1969, *J. Phys. B: At. Mol. Phys.*, **2**, 107.
Martin, N.L.S.: 1984, *J. Phys. B: At. Mol. Phys.*, **17**, 1797.
Martin, W.C., Sugar, J. and Tech, J.L.: 1972, *J. Opt. Soc. Am.*, **62**, 1488.
Mies, F.H.: 1968, *Phys. Rev.*, **175**, 164.
Panajotivić, R.: 1999, PhD Thesis, Faculty of Physics, University of Belgrade.
Panajotović, R., Pejčev, V., Konstantinović, M., Filipović, D., Bočvarski, V. and Marinković, B.: 1993, *J. Phys. B: At. Mol. Opt. Phys.*, **26**, 1005.
Panajotović, R., Šević, D., Pejčev, V., Filipović, D.M. and Marinković, B. P.: 2004, *Int. J. Mass Spectrom.*, **233**, 253.
Predojević, B., Šević, D., Pejčev, V., Marinković, B.P. and Filipović, D.M.: 2003, *J. Phys. B: At. Mol. Opt. Phys.*, **36**, 2371.
Ross, K. and Sonntag, B.: 1998, *Rev. Sci. Instrum.*, **66**, 4409.
Stevanović, Lj., Marinković, B.P. and Filipović, D.M.: 2003, Proc. 5th Balkan Physical Union Conference (BPU-5), Vrnjačka Banja, Serbia and Montenegro, August 25 29, Book of Abstracts, Eds. S. Jokić, I. Milošević, A. Balaž, Z. Nikolić, (Belgrade: Serbian Physical Society), p. 293. `http://www.phy.bg.ac.yu/ bpu5/proceedings/Papers/SP04%20-%20007.pdf`
Trajmar, S. and Williams, W.: 1976, Proc. VIII SPIG Physics of Ionized Gases Ed. Novinšek, B. (Ljubljana: University of Ljubljana Press), p. 199.

ЕЛЕКТРОНСКА СПЕКТРОСКОПИЈА АУТОЈОНИЗАЦИОНИХ СТАЊА ЦИНКА

B. Predojević[1,2], D. Šević[1], V. Pejčev[1,3], B. P. Marinković[1] and D. M. Filipović[1,4]

[1] *Institute of Physics, PO Box 57, 11001, Belgrade, Serbia and Montenegro*

[2] *Faculty of Natural Sciences, University of Banja Luka, Republic of Srpska, Bosnia and Herzegovina*

[3] *Faculty of Natural Sciences, University of Kragujevac, Serbia and Montenegro*

[4] *Faculty of Physics, University of Belgrade, PO Box 368, 11001, Belgrade, Serbia and Montenegro*

UDK 52.47
Оригинални научни рад

Спектри губитака енергије аутојонизационих стања атома цинка су снимљени у енергијском интервалу од 10,8 до 12,5 eV, за енергије упадних електрона од 20 до 100 eV, и за углове расејања од 0° до 10°. Извршена је декомпозиција спектара употребом χ^2 минимализационе процедуре да би се показао допринос прелаза из унутрашње љуске типа $3d^{10}4s^2 \rightarrow 3d^9 4s^2 4p$. Релативни интензитети прелаза су одређени у односу на интензитет резонантног прелаза $3d^{10}4s^2 \rightarrow 3d^{10}4s4p$. Разматрани су облик и ширина линија. Резултати су упоређени са другим експерименталним мерењима и теоријским проценама.